S1051-2004(05)00090-4/FLA AID:588 Vol.●●●(●●●) ydspr588 [DTD5] P.1 (1-20)
YDSPR:m1a v 1.42 Prn:3/08/2005; 10:48 by:Vita p. 1

Available online at www.sciencedirect.com
SCIENCE DIRECT®

ELSEVIER

Digital Signal Processing ●●● (●●●●) ●●●–●●●

Digital Signal Processing

www.elsevier.com/locate/dsp

New anti-jamming technique for GPS and GALILEO receivers using adaptive FADP filter ☆

René Landry Jr. *, Pierre Boutin, Aurelian Constantinescu

Ecole de Technologie Supérieure, Montreal, QC H3C 1K3, Canada

Abstract

Anti-jamming techniques to improve global positioning system (GPS) receiver's robustness have been mainly developed in military applications. None of civilian techniques can procure sufficient robustness against occasional or intentional jammers for civil GPS or GALILEO navigation receivers. The amplitude domain processing (ADP) filtering is a technique based upon Capon works and Neyman–Pearson theory. Several experiments concerning the ADP filtering have been considered at the 3DETSNAV division of LACIME laboratory at Ecole de Technologie Supérieure (ETS), which have proved that the technique is reliable in order to eradicate powerful interference present in the spread spectrum signal. However, the results show that the ADP filter has a real limitation when submitted to multiple interference scenarios. This paper shows that working in the frequency domain is more efficient because jamming signals added to a white Gaussian noise are easier to detect and to attenuate when represented in the frequency domain. The present paper gives mathematical elements to complete the ADP theory in the frequency domain and presents the performances of an ADP in the frequency domain (FADP) filter simulated in a Matlab Simulink environment. The filter is tested with a signal composed of a GPS C/A code (Gold sequence) drowned in a white Gaussian noise in presence of one or several additional jammers (CWI, PWI, chirp). Several analyses are made upon the filter output (signal to noise ratio, attenuation and power spectral density measurements). The results of the analysis show that the FADP can eradicate any kind of jammers of 20 dB above white Gaussian noise. Correlation losses are measured; they are always under 0.5 dB. In the presence of one or two jammers, the performances of the FADP filter are better than those of the ADP filter. The FADP filter

☆ This work was supported by Natural Sciences and Engineering Research Council of Canada (NSERC) and Fonds de Recherche sur la Nature et les Technologies (FCAR), along with CMC Electronics.

* Corresponding author. Fax: +514 396 8684.
E-mail addresses: rlandry@ele.etsmtl.ca (R. Landry), pboutin@ele.etsmtl.ca (P. Boutin), aconstan@ele.etsmtl.ca (A. Constantinescu).

1051-2004/$ – see front matter
doi:10.1016/j.dsp.2005.04.015

S1051-2004(05)00090-4/FLA AID:588 Vol.●●●(●●●) ydspr588 [DTD5] P.2 (1-20)
YDSPR:m1a v 1.42 Prn:3/08/2005; 10:48 by:Vita p. 2

can procure up to 20 dB processing gain with a maximum of 10 dB loss on SNR in worse jamming scenario. When the number of jammers increases, the performances remain convenient, whereas the time-domain ADP filter becomes unable to be effective. In this paper, measurements are made with a number of jammers up to 15.

Keywords: Adaptive filtering; CDMA anti-jamming; FADP; GPS; GALILEO; Simulink model

1. Introduction

Interference perturbations are of real concern for navigation systems. In the case of low-power interference, anti-jam techniques are not always necessary because of spectral spreading, currently used in navigation systems, which will significantly attenuate the effect of the jammers. But as soon as the power of the interference becomes more important, it is really useful to appeal to anti-jam techniques. Reference [1] gives a thorough study of the impact of jamming upon the capacity to detect the correct information with a global positioning system (GPS) receiver. Nevertheless, for the last twenty years, only few anti-jamming techniques were developed and implemented in GPS receivers in order to improve data detection, except for military applications. Pre-correlation techniques, used before the stage of correlation, and post-correlation techniques used to improve the signal quality after the correlation stage can be distinguished. Several of them are evocated in [2].

Adaptive radiation chart antenna or fixed bandpass filtering can be considered in a receiver before the correlation stage and may eradicate interference in far frequencies. In multi-standard receivers capable of receiving both GPS and global navigation satellite system (GLONASS) signals, these techniques have some difficulties to detect jammers whose frequency ranges are located between the GPS and GLONASS bands [3]. Other pre-correlation techniques perform better results, like the use of an automatic gain control (AGC) with an adaptive analog digital converter (ADC), as presented in [4]. One can also mention digital techniques to reject interference in the frequency range of the useful signal. They have the capability to be used at low cost with some minor modifications and high efficiency. For example, adaptive spectral filtering consists in detecting interference peaks in the signal spectrum and inserting at the exact location of the jammer a stopband filter in order to attenuate the main power of the signal. Another example is the Piranha filter, composed with a succession of adaptive notch filters which has been the target of a thorough study in [2,5].

Numerous techniques of post-correlation can also turn out to be useful to reject wide band Gaussian interference. The extended range correlator, presented in [6,7], maintains the code synchronization when tracking loop errors exceed values that can be tolerated by a standard correlator.

The amplitude domain processing (ADP) is based upon Capon works [8] and Neyman–Pearson theory [9]. This technique is fully adaptive and completely digital, allowing easy implementation and high efficiency when jammers are located in the useful signal band. Unfortunately, very few papers are devoted to ADP filtering, which has proven to be a reliable technique to eradicate powerful interference applied to a spread spectrum signal.

S1051-2004(05)00090-4/FLA AID:588 Vol.●●●(●●●) ydspr588 [DTD5] P.3 (1-20)
YDSPR:m1a v 1.42 Prn:3/08/2005; 10:48 by:Vita p. 3

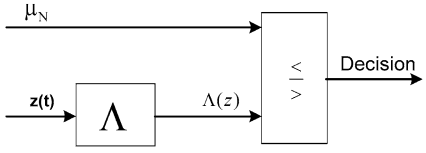

Fig. 1. Probability ratio concept, as referred to Neyman–Person and Capon works.

Reference [7] presents the results obtained in experiments on GPS P code, while Refs. [6,10,11] show simulation results on coarse/acquisition (C/A) GPS code. But the main drawback of ADP filtering, as shown in [7,11] is the incapability to resist to scenarios having more than two simultaneous interferences.

Indeed, the ADP filter is really transparent to white Gaussian noise and to spread-spectrum navigation signals, by the same way allowing no deterioration of those signals. For example, when 3 or 4 different jammers are present in the spectrum, the resulting probability density function (PDF) tends to a Gaussian characteristic. Consequently, a temporal ADP filter becomes unable to differ multiple interference from Gaussian noise. Because most of interference is concentrated around a specific frequency range, the digital signal processing in the frequency domain will be more efficient. Multiple interference will be easier to detect because its spectrum is completely different from the white Gaussian noise spectrum. Thus, after briefly reminding the principles of the ADP theory, this paper presents the differences between the spectral and the temporal ADP theories. Then the whole structure of the ADP in the frequency domain (FADP) filter and the way it can be inserted in a standard GPS receiver will be presented in detail. The last part of this paper is aimed to expose the performances of the FADP filter and to compare the results with those obtained using a temporal ADP filter.

2. Theoretical basis of the FADP filter

The ADP technique is based upon Capon work [8] and statistical theory of Neyman–Pearson [9]. The main objective is to evaluate a probability ratio $\Lambda(x)$, as function of the samples of signal $z(t)$, as statistically demonstrated in [12]. The presence or the absence of the signal is determined by comparing this ratio to a decision threshold μ_N (see Fig. 1).

This method is optimum insofar as the error probability (the probability to detect a signal whereas there is no signal or not to detect a signal whereas there is one) is minimized. First, the ADP filter theory will be elaborated. For more details, the reader could refer to [11,13,14]. Then, mathematical developments will be performed for the spectral representation version of the ADP.

2.1. Elaboration of the ADP theory

The basis of this section can be found in [11], where some further elaborations have been considered. The same notation for the GPS signal application will be used in all this

S1051-2004(05)00090-4/FLA AID:588 Vol.●●●(●●●) ydspr588 [DTD5] P.4 (1-20)
YDSPR:m1a v 1.42 Prn:3/08/2005; 10:48 by:Vita p. 4

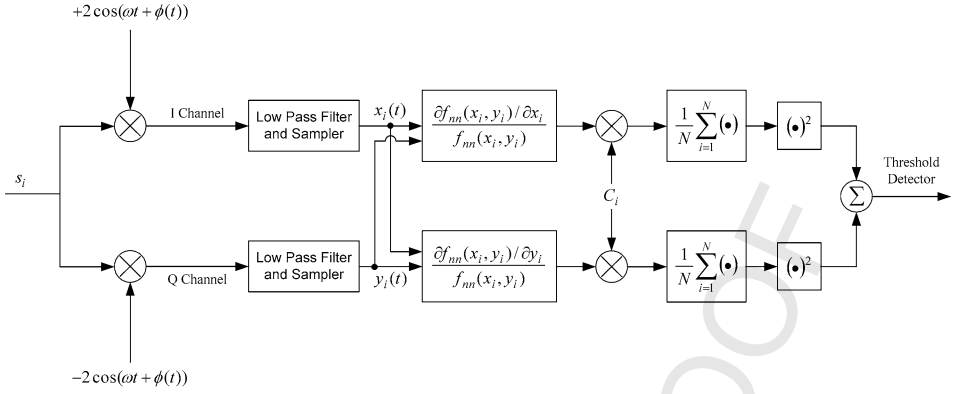

Fig. 2. Optimized theoretical receiver in rectangular coordinates.

paper. The signal captured by the GPS receiver can be written as following:

$$z(t) = r(t,\theta) + w(t), \tag{1}$$

$$r(t,\theta) = s(t)\cos(\omega t + \theta), \tag{2}$$

where $r(t)$ is the modulated information, $s(t)$ is the useful data, and $w(t)$ is a white Gaussian noise including potential interference. The detection problem is to decide between $z(t) = r(t,\theta) + w(t)$ and $z(t) = w(t)$, when the signal is absent.

After extraction of the base band quadrature components, the detection problem is to decide between $x_i = s_i\cos\theta + n_{xi}$; $y_i = s_i\sin\theta + n_{yi}$ and $x_i = n_{xi}$; $y_i = n_{yi}$.

Let

$$f_{nn}(x,y) = \sum_{i=1}^{N} f_{nn}(x_i, y_i)$$

be the input PDF of $z(t)$. It can be shown that this function is equal to the noise PDF. According to [13], the optimal probability ratio evocated in Fig. 1 can be written as following:

$$\Lambda(w_x, w_y) - 1 = \left[\frac{1}{N}\sum_{i=1}^{N} s_i \frac{\partial f_{nn}(x_i, y_i)/\partial x_i}{f_{nn}(x_i, y_i)}\right]^2 + \left[\frac{1}{N}\sum_{i=1}^{N} s_i \frac{\partial f_{nn}(x_i, y_i)/\partial y_i}{f_{nn}(x_i, y_i)}\right]^2, \tag{3}$$

for a N-sampled complex signal, where x and y represent the real and imaginary parts of the signal $z(t)$, w_x and w_y are the real and imaginary parts of the noise $w(t)$ and s_i represents the samples of the signal $s(t)$. This formula, represented in Fig. 2 (see [13]), can be easily used in a conventional receiver to achieve its optimum form. Equation (3) has been obtained by making use of the small-signal assumption and by using an expansion of f_{nn} in a Taylor series around the values of the received data (x_i, y_i).

The drawback of the representation (3), while optimum, is that it is necessary to apply a non-linear function upon the two channels I and Q (in phase and in quadrature, respectively), which doubles the required resources. Moreover, we need a perfect knowledge of

S1051-2004(05)00090-4/FLA AID:588 Vol.●●●(●●●) ydspr588 [DTD5] P.5 (1-20)
YDSPR:m1a v 1.42 Prn:3/08/2005; 10:48 by:Vita p. 5

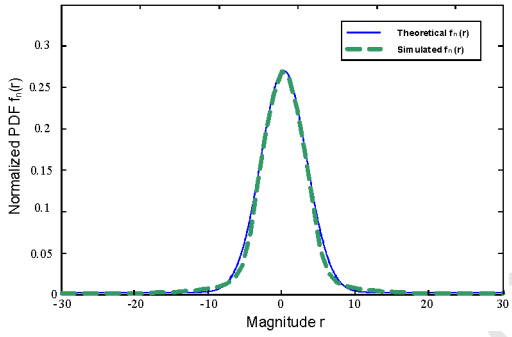

Fig. 3. Theoretical and simulated $f_n(r)$ of a white Gaussian noise ($N = 2048$).

the joint I and Q noise PDF and fast hardware to compute twice partial derivatives. According to [14], it is possible to work in polar coordinates, because noise and signal carrier are not synchronized. Hence, the probability ratio (3) becomes

$$\Lambda(w_x, w_y) - 1 = \frac{1}{N^2}\sum_{i=1}^{N}\left[s_i g_r(r_i)\right]^2\left[\frac{(x_i^2 + y_i^2)}{r_i^2}\right] = \left[\frac{1}{N}\sum_{i=1}^{N} s_i g_r(r_i)\right]^2, \tag{4}$$

where

$$g(r_i) = \frac{\partial/\partial r_i\,(f_n(r_i)/r_i)}{f_n(r_i)/r_i} = \frac{\partial}{\partial r_i}\ln\frac{f_n(r_i)}{r_i}. \tag{5}$$

With this amplitude representation a new non-linear function $g(r)$ is introduced, where $f_n(r)$ is the radial PDF of the useful signal amplitude r. In the absence of interference, $f_n(r)$ is a Gaussian distribution because a Gaussian noise has a circular symmetry and its phase is uniformly distributed. The relation between both representations of PDF $f_n(r)$ and $f_{nn}(x, y)$ (polar and rectangular representations, respectively) is:

$$f_n(r_i) = 2\pi r_i f_{nn}(x, y). \tag{6}$$

For a white Gaussian noise, $f_n(r)$ has a Gaussian shape as shown in Fig. 3, where the theoretical and simulated values are presented. The theoretical curve has been obtained by using the corresponding mathematical representation of $f_n(r)$, the simulated one by simulation of a white Gaussian noise.

This result is useful because it enables to apply this function to the signal module where the phase is not modified, but only delayed. This polar structure can be represented as in Fig. 4 (see [14]).

The examination of this function, $g(r)$, is mainly interesting for the CDMA signals. When a Gaussian PDF signal of the form

$$f_n(r) = Ae^{-r^2/2} \tag{7}$$

is applied at the input, $g(r)$ given by (5) may be written as

$$g(r) = r + \frac{1}{r}. \tag{8}$$

S1051-2004(05)00090-4/FLA AID:588 Vol.●●●(●●●) ydspr588 [DTD5] P.6 (1-20)
YDSPR:m1a v 1.42 Prn:3/08/2005; 10:48 by:Vita p. 6

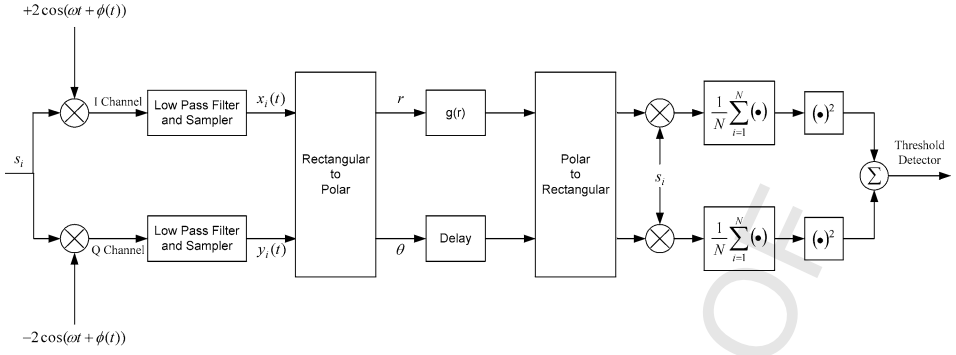

Fig. 4. Optimized theoretical receiver in polar coordinates.

This result is really significant because $g(r)$ has a linear form (except near 0), which let suppose that it remains white Gaussian noise unchanged, in its linear zone. Practically, the real calculation is slightly different because the division by 0 is likely to introduce errors. For this reason, a modified version of the $g(r)$ definition is proposed as

$$g(r) = -\frac{\partial}{\partial r} \ln \frac{f_n(r)}{\alpha r + \beta}. \tag{9}$$

If a translation and a rescale of the magnitude axis r is considered, using the same example as above (7), the real form of $g(r)$ is

$$g(r) = r + \frac{\alpha}{\alpha r + \beta}. \tag{10}$$

Hence, we only have to make a good choice of α and β to make the second term of $g(r)$ negligible (e.g., $\alpha = 0.08$ and $\beta = 110$). Another delicate point of the computation of $g(r)$ is to have a null or negative argument of the logarithm. To avoid negative values, the magnitude range can be translated toward greater values in order to have only positive values of r, then $f_n(r)/r \geqslant 0$. To avoid null values, it is necessary to add a small positive constant k to $f_n(r)$. The resulting $g(r)$ function becomes

$$g(r) = -\frac{\partial}{\partial r} \ln \frac{f_n(r) + k}{\alpha r + \beta}. \tag{11}$$

With a Gaussian input signal (7), one finally obtains

$$g(r) = \frac{r}{1 + k e^{r^2/2}/A} + \frac{\alpha}{\alpha r + \beta}. \tag{12}$$

If a small k is chosen, (12) is similar to (10). The graphical effect of this precaution upon the aspect of $g(r)$ function can be seen in Fig. 5. The final value of k is 0.001.

2.2. Theoretical aspects of the FADP techniques

As shown in Fig. 6, the FADP filter theory remains the same as the ADP theory (see Section 2.1) except the fact that it is now applied to the frequency samples instead of being applied to the time domain amplitude. The same notations can be used, and r becomes the

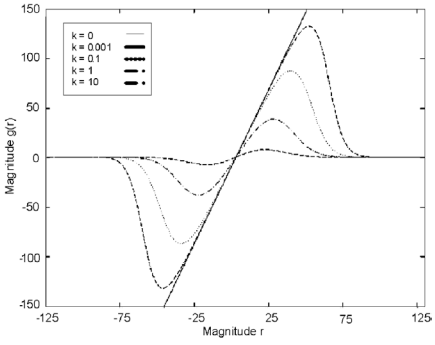

Fig. 5. $g(r)$ function appearance when submitted to a white Gaussian noise (different values of k and $A = 1$).

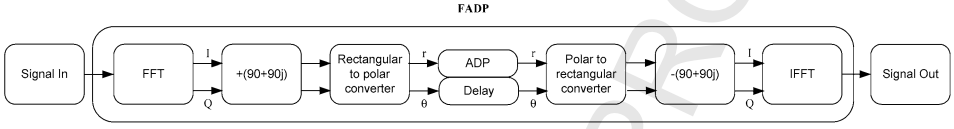

Fig. 6. Global diagram of the FADP filter.

spectrum amplitude (function of frequency instead of time). $f_n(r)$ becomes the joint PDF of the frequency decomposition of I and Q. Several precisions have to be brought because the situation is slightly different in various points.

The ADP filter can be implemented for a real or a complex signal. In the case of a real signal, the situation is simpler because it is sufficient to apply the $g(r)$ function to the real signal. In the case of a complex signal, it is necessary to transform the rectangular to polar coordinates. In the configuration of the FADP filter, the FFT block is a core delivering a two-channels signal so only the second (complex) situation is envisioned.

In a GPS receiver, the useful signal is spread over white Gaussian noise with zero mean value. The noise PDF (real and complex) remains Gaussian-shaped centered on 0 after the FFT block, but its shape is modified when converted to polar coordinates. Consider I and Q the rectangular complex channels and R, the complex module, with $R = \sqrt{I^2 + Q^2}$ (see Fig. 6). For a Gaussian noise

$$f_n^I(r) = f_n^Q(r) = \frac{A}{\sqrt{2\pi}} e^{-r^2/2} \tag{13}$$

and the two following statistic properties can be used

$$f_n^{I^2}(r) = f_n^I(\sqrt{r})/\sqrt{r}, \tag{14}$$

$$f_n^{(I^2+Q^2)}(r) = f_n^{I^2}(r) * f_n^{Q^2}(r), \tag{15}$$

where $*$ represents the convolution product.

According to (14), we have

$$f_n^{I^2}(r) = (A/\sqrt{2\pi r}\,)\exp(-r/2). \tag{16}$$

S1051-2004(05)00090-4/FLA AID:588 Vol.●●●(●●●) ydspr588 [DTD5] P.8 (1-20)
YDSPR:m1a v 1.42 Prn:3/08/2005; 10:48 by:Vita p. 8

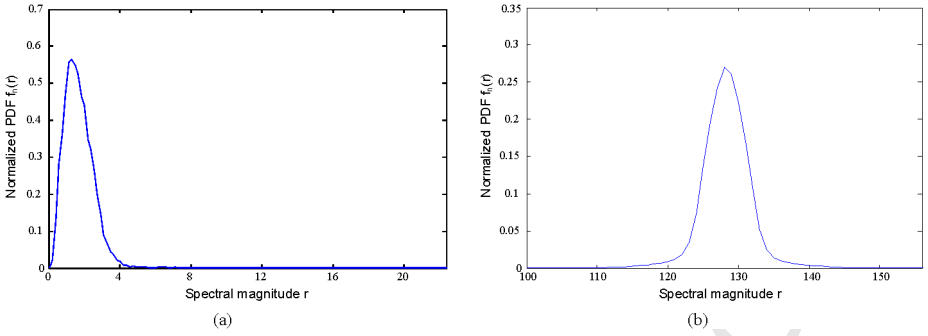

Fig. 7. Example of $f_n(r)$ appearance without (a) and with (b) the additional complex constant, $C = 90(1+i)$.

Then, using (15),

$$f_n^{(I^2+Q^2)}(r) = \left[(A/\sqrt{2\pi r})\exp(-r/2)\right] * \left[(A/\sqrt{2\pi r})\exp(-r/2)\right]. \tag{17}$$

If we develop the convolution, the following integral must be evaluated:

$$f_n^{(I^2+Q^2)}(u) = \int_0^u \left[(A/\sqrt{2\pi r})\exp(-r/2)\right]\left[\left(A'/\sqrt{2\pi(u-r)}\right)\exp(-(u-r)/2)\right] dr. \tag{18}$$

We made the following variable change

$$x = r - \frac{u}{2}, \tag{19}$$

and (18) becomes

$$f_n^{(I^2+Q^2)}(u) = (AA'/2\pi)\exp(-u/2)\ln(1+\sqrt{2}) = K\exp(-u/2), \tag{20}$$

where K is a constant. With the use of (14), we have

$$f_n^{\sqrt{(I^2+Q^2)}}(r) = Kr\exp(-r^2/2). \tag{21}$$

Consequently, the development shows that a chi square-shaped PDF is obtained at the output of the FFT instead of a Gaussian distribution. The filter does not remain linear anymore with an input having a chi square-shaped PDF. Using (9) to compute the $g(r)$ function, the following formula is obtained with a chi square-shaped $f_n(r)$:

$$g(r) = -\frac{\partial}{\partial r}\left[-r^2/2 + \ln r + \ln K - \ln(\alpha r + \beta)\right] = r - \frac{\beta}{r(\alpha r + \beta)}. \tag{22}$$

The $g(r)$ function in frequency domain diverges around 0. Therefore, it is useful to transform properly the FFT block output signal to obtain the original Gaussian form of $f_n(r)$. The solution adopted is to simply add a complex constant C to the output of the FFT block, which translates the spectral PDF on the spectral magnitude axis (see Fig. 7).

S1051-2004(05)00090-4/FLA AID:588 Vol.●●●(●●●) ydspr588 [DTD5] P.9 (1-20)
YDSPR:m1a v 1.42 Prn:3/08/2005; 10:48 by:Vita p. 9

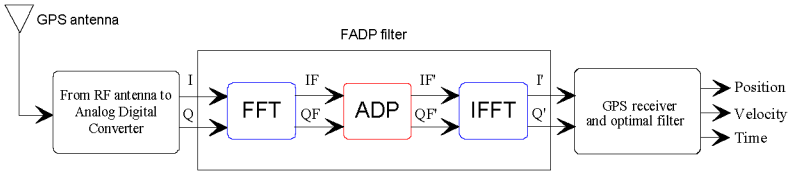

Fig. 8. Example of the easy "plug-in" FADP filter, inserted in a GPS receiver architecture.

The consequence to add this complex constant is to translate the calculated module around the $|C|$ value. If $C = 90 + 90i$ is chosen, the convolution calculated in (17) becomes:

$$f_n^{(I^2+Q^2)}(r) = \left[(A/\sqrt{2\pi r})\exp(-(r-90)/2)\right] * \left[(A/\sqrt{2\pi r})\exp(-(r-90)/2)\right]. \tag{23}$$

As shown in Fig. 7b, the Gaussian symmetry is kept if we choose a constant sufficiently far from 0.

3. Architecture of the FADP filter inserted in a GPS, GALILEO, or CDMA receiver

The main interest to work in the frequency domain is to obtain a better control upon jammers. In the case of more than two jammers, the ADP filter has difficulties to differ jammers from the Gaussian noise. This results in a more important residual power of the interference transmitted through the filter. In the case of the FADP filter, a spectral processing enables to manage each jammer independently, which is more efficient.

As explained above, the FADP filter is mainly an adaptive ADP filter working in the frequency domain. One of the advantages of digital anti-jamming filters is that they are "plug-in" filters, meaning that they do not require complex operations in order to be inserted in a GPS architecture (see Fig. 8). So first, let us concentrate our attention to the FFT and inverse fast Fourier transform (IFFT) blocks considered before and after the filter and then, we will describe in detail the architecture of the ADP filter, using the theory developed previously. The global structure of the FADP filter is presented in Fig. 8.

3.1. The FFT and IFFT blocks

Before the ADP filter (see Fig. 9), a FFT block is used to compute the input signal spectrum. Then a complex constant C is added to the signal, as explained in Section 2.2 and a rectangular to polar converter block enables to work on the signal module. Afterwards, this constant will be set to $C = 90(1 + j)$, because the input spectral signal is centered in $|90(1 + j)| \approx 127$, instead of being centered in 0. Using a 8-bits analog to digital converter (ADC), 127 is an interesting value because the useful signal can be coded between 0 and 256. The complementary operations are done at the output of the ADP filter in order to recover a rectangular spectral signal and then, a temporal signal (the IFFT block).

The FFT and IFFT blocks are classical ones, using the FFT algorithm, whose main advantage is the ability to compute a Fourier transform with a complexity of $N \log N$ instead

S1051-2004(05)00090-4/FLA AID:588 Vol.●●●(●●●) ydspr588 [DTD5] P.10 (1-20)
YDSPR:m1a v 1.42 Prn:3/08/2005; 10:48 by:Vita p. 10

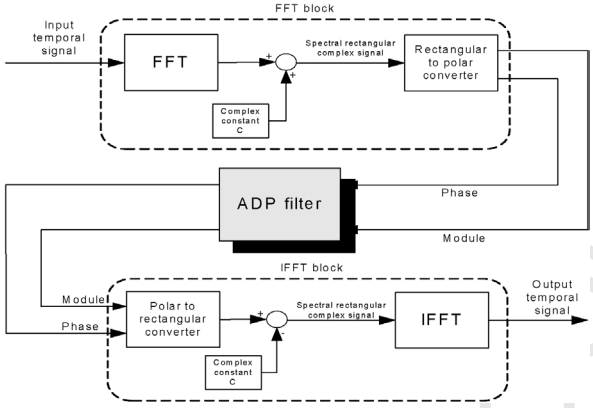

Fig. 9. Global implementation of the FADP filter.

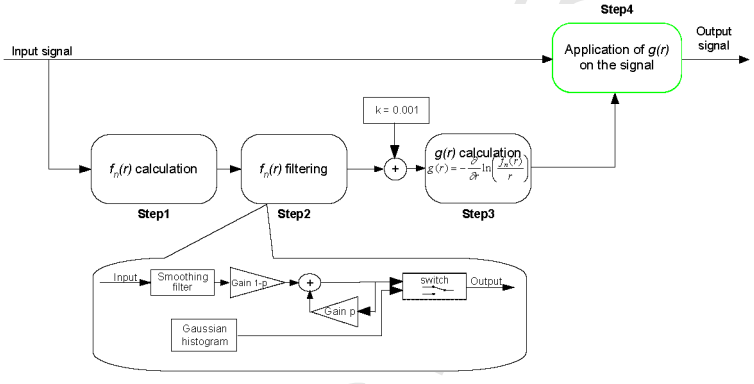

Fig. 10. Global schematic view of the ADP filter.

of N^2 for a classical discrete Fourier transform (DFT), where N is the size of the vectors submitted to the FFT and IFFT blocks. For the present application, we have chosen $N = 256$.

3.2. Structure of the ADP filter

The ADP filter used in the frequency domain remains close from the temporal ADP filter structure, which is described in [10,11]. This section will bring some additional details concerning the functioning of the filter in the frequency domain.

As shown in Fig. 10, there are four significant steps in the architecture implementation of an ADP filter. In the first step, a histogram $f_n(r)$ of the input signal is computed. Before calculating the $g(r)$ function (using (5)), a filter block is inserted to smooth the real-time histogram; this is the second step of the ADP architecture implementation. It contains a FIR filter (smoothing filter), whose output is determined from the input using the following expression:

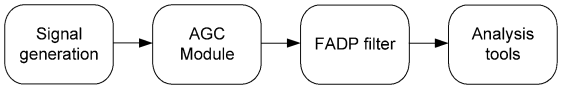

Fig. 11. Global testing environment for the FADP filter.

$$s_{\text{out}}(i) = 0.125s_{\text{in}}(i-3) + 0.125s_{\text{in}}(i-2) + 0.125s_{\text{in}}(i-1) + 0.25s_{\text{in}}(i) + 0.125s_{\text{in}}(i+1) + 0.125s_{\text{in}}(i+2) + 0.125s_{\text{in}}(i+3). \quad (24)$$

As the ADP filter is adaptive, it is able to react immediately to a change of the input signal (e.g., brutal apparition of interference). But a severe change of the $f_n(r)$ function would entail a brutal change of the $g(r)$ function and of the output signal. Consequently, the filter also contains a loop to avoid discontinuities in the case of important changes in the input signal. This loop is introduced in the filter block. It is possible to make it more or less stronger, by changing the gain percentage (the p value in Fig. 10). In order to accelerate the convergence of the loop, it can be initialized with a Gaussian output function at the beginning of the signal acquisition.

A small constant k ($k = 0.001$ has been chosen here) is added at the output of the $f_n(r)$ function. This is made just before the calculation of $g(r)$, which represents the third step of the ADP filter architecture implementation, in order to avoid computation problems (e.g., $\ln(0)$), as explained in Section 2.1. Then the $g(r)$ function is computed and applied to the input signal. The application of the $g(r)$ function to the signal is the last step of the ADP block implementation. The main difference between the FADP filter and the temporal ADP filter is the following one: it is necessary to take care of the central value of the output signal, which is set to 127 instead of 0. The $f_n(r)$ and $g(r)$ functions are also centered around 127 and the image of the $g(r)$ function must be centered on 127, instead of 0, to create an output of the filter centered in 127. Thus, the $g(r)$ function must be slightly changed in the simulations, compared to [10,11], in order to shift the output signal.

4. Simulation of the FADP filter in a Simulink environment

In order to evaluate the ADP vs FADP filter performances, we need to build a testing simulator (see Fig. 11). A GPS like signal is applied to an automatic gain control (AGC), who normalizes the power of the signal. Next the signal is applied to the FADP filter for further performance analysis. First, we will deal with the signal source composition. Then, we will develop every means used to make performance measurements.

4.1. Signal generation

The input signal used in the simulator is a GPS C/A (coarse acquisition) code, created with Gold code generators G1 and G2 (see Fig. 12a). This Gold code is a periodic sequence of 1023 chips evolving at a rate of 1.023 Mchips/s. Thus, the period of this pseudo-random noise sequence lasts 1 ms. The GPS satellites can use 37 orthogonal pseudo random sequences and the simulator can select any of them. The phase selector in Fig. 12a will determine which satellite is chosen for the simulation. Figure 12b shows the frequency

S1051-2004(05)00090-4/FLA AID:588 Vol.●●●(●●●) ydspr588 [DTD5] P.12 (1-20)
YDSPR:m1a v 1.42 Prn:3/08/2005; 10:48 by:Vita p. 12

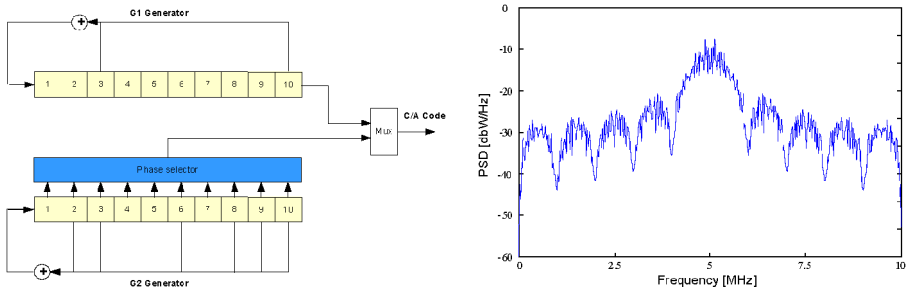

(a) (b)

Fig. 12. Synthesis of the C/A-code (a) and associated 5 MHz IF spectrum obtained with a sampling rate of 20 Msamples/s (b).

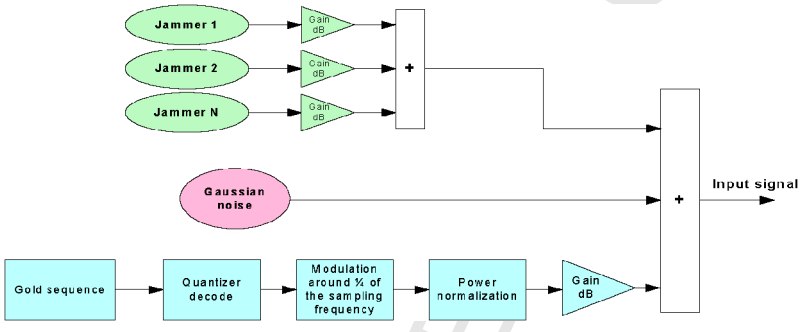

Fig. 13. General structure of the simulator input signal.

spectrum of the Gold code centered at the intermediate frequency (IF) of 5 MHz (power of 0 dB W). Additive white Gaussian noise (AWGN) is added to the GPS signal along with several kinds of jammers. Simple gains (in dB) enable to calibrate the jammers and the useful data JNR and SNR, respectively. Figure 13 shows a schematic view of the entire signal submitted to the simulator.

In order to consider the main jamming scenarios of the GPS signal, three types of jammers have been considered:

- Continuous wave interference (CWI). It is one of the most frequently encountered jamming signals, representing RF spikes, which could appear at any time in the spectrum. The spectral representation of the CWI jammer is presented in Fig. 20a.
- Pulsed wave interference (PWI). It corresponds mainly to signals emitted by RADAR stations. The temporal and spectral representations of a PWI jammer are presented in Figs. 14 and 21a, respectively.
- Chirp interference. It is a sinusoid interference including Doppler shift effect (variation of the frequency in time). The spectrum of such a signal is spread on the frequency range covered by the signal due to the FFT time process. The temporal and spectral representations of a chirp jammer are presented in Figs. 15 and 22a, respectively.

S1051-2004(05)00090-4/FLA AID:588 Vol.●●●(●●●) ydspr588 [DTD5] P.13 (1-20)
YDSPR:m1a v 1.42 Prn:3/08/2005; 10:48 by:Vita p. 13

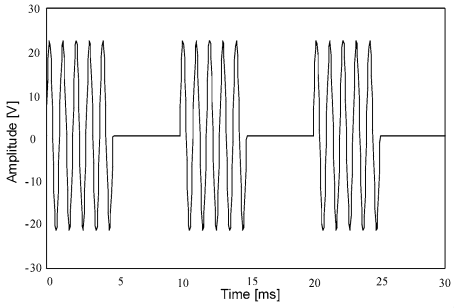

Fig. 14. Temporal representation of a PWI jamming signal with a 50% duty cycle (JNR = 20 dB, noise at 0 dB W).

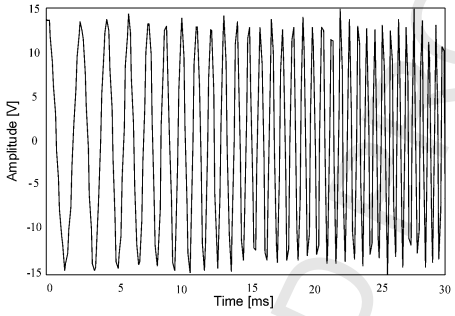

Fig. 15. Temporal representation of a Chirp jamming signal (frequency between 5 and 7.5 MHz, JNR = 20 dB, noise at 0 dB W).

Several preliminary studies have been carried out upon the global source to verify the impact of jammers on the GPS signal. GPS correlation losses (difference between correlation in absence and presence of a jamming signal) are measured, first in the presence of a notch filter moving in the spectrum and finally in the presence of a CWI jammer. These results are shown in Fig. 16 (sampling frequency of 20 Msamples/s). When a notch filter is centered in the main lobe of the GPS signal centered at 5 MHz, the correlation loss is significant because of the GPS signal structure (see Fig. 16a). This is the main reason why a jammer whose frequency is located in the main lobe of the GPS signal (where 95% of its power can be measured) affects the most GPS reception. Figure 16b emphasizes the link existing between JNR and correlation loss, which shows the impact generated by increasing the amplitude of the jamming signal.

4.2. Description of the analysis tools

To evaluate the FADP filter performances in simulation, the power ratio measurements and the power spectral density (PSD) have been used. The definition of every ratio will be reminded to clarify the following analysis. In the simulator, the input signal can be considered as in (1), with $w(t)$ not necessarily a white Gaussian noise:

$$w(t) = n(t) + j(t), \tag{25}$$

S1051-2004(05)00090-4/FLA AID:588 Vol.●●●(●●●) ydspr588 [DTD5] P.14 (1-20)
YDSPR:m1a v 1.42 Prn:3/08/2005; 10:48 by:Vita p. 14

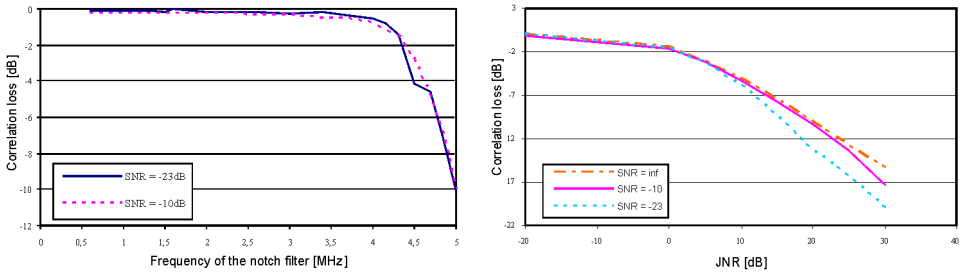

Fig. 16. (a) Correlation loss when GPS signal crosses a notch filter. (b) Correlation loss as function of the JNR of a CWI.

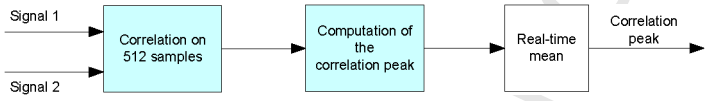

Fig. 17. Computation of the real-time mean of crosscorrelation peak.

where $n(t)$ is the white Gaussian noise considered above and $j(t)$ is the sum of all jamming signals. Using these notations, two ratios are computed, based on correlation measurements, as shown in [13]:

$$\text{SNR} = \sigma_s^2/\sigma_n^2 \quad \text{and} \quad \text{JNR} = \sigma_j^2/\sigma_n^2, \tag{26}$$

where σ_s^2, σ_n^2, and σ_j^2 are the powers of $s(t)$, $n(t)$, and $j(t)$, respectively (the variances of the signal, noise and jammers).

The main problem of the correlation peak computation lies in the fact that this measurement needs a lot of signal samples (usually few C/A code periods) to have consistent correlation measurements. A sample rate of 20 Msamples/s was chosen in the simulator. A good measurement would need at least $20 \times 1023 = 20{,}460$ samples (which is equivalent to 1 ms period of the Gold sequence), resulting in a large processing time. Consequently, it was decided to organize the calculation differently, as shown in Fig. 17. The correlation peak is computed with only 512 samples and a real-time mean block enables to obtain the mean of an important number of peaks (100 or more). Moreover, it is possible to reinitialize the mean block whenever. Thus, when the average is computed with more than 100 correlation peaks, resulting measurement is surely reliable.

If a complex signal s composed of GPS data $gps(t)$ and an important white Gaussian noise $n(t)$ are considered,

$$s(t) = gps(t) + n(t) \tag{27}$$

the crosscorrelation between s and the GPS signal is written as

$$c_l = \sum_{i=0}^{N-1} s_i gps_{i-k} = \sum_{i=0}^{N-1} (gps_i + n_i) gps_{i-k} \quad \text{with } -N \leqslant l \leqslant N, \tag{28}$$

S1051-2004(05)00090-4/FLA AID:588 Vol.●●●(●●●) ydspr588 [DTD5] P.15 (1-20)
YDSPR:m1a v 1.42 Prn:3/08/2005; 10:48 by:Vita p. 15

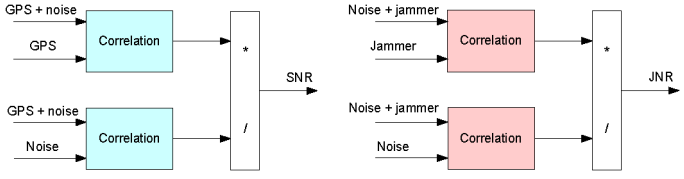

Fig. 18. Calculation of SNR and JNR ratios.

and

$$c_0 = \sum_{k=0}^{N-1} gps_k^2 + \sum_{k=0}^{N-1} gps_k n_k. \tag{29}$$

We can see that the crosscorrelation is finally the sum of the autocorrelation of the GPS signal and the crosscorrelation between the GPS signal and the Gaussian noise. If we consider the correlation peak given by (29), obtained for $l = 0$, the first term is the GPS signal power and the second one is mainly zero, because the crosscorrelation between noise and GPS data is a noise floor close to 0. Then the result of the crosscorrelation is close to the GPS signal power.

In the simulator, each signal power can be computed independently because crosscorrelation terms are always negligible: useful data signal is really weak compared to the noise power, so crosscorrelation between useful data and noise can be neglected. For the JNR calculation, the jammer power is supposed to be weak at the output of the FADP filter so the crosscorrelation between jam and noise is negligible too. Consequently, the values obtained are reliable. If we are able to evaluate the GPS signal power and, with the same method, the noise and jammers powers, we are able to compute the output SNR and JNR. These data are obtained by computing the ratio between different correlation peaks, as shown in Fig. 18.

The SNR and JNR measurements give precious information concerning the quality of the output signal. With this information, we can compute processing gain and SNR loss defined as

$$\text{processing gain} = \text{JNR}_{\text{in/dB}} - \text{JNR}_{\text{out/dB}}, \tag{30}$$

$$\text{SNR loss} = \text{SNR}_{\text{out/dB}} - \text{SNR}_{\text{in/dB}}. \tag{31}$$

The processing gain characterizes the ability to eradicate jammers and the correlation loss represents the ability to keep original useful signal unchanged.

In parallel, the power spectral density (PSD) is a discrete function of the frequency, as shown below:

$$P(m\nu_0) = \left[\frac{1}{NT_s} \left| \sum_{i=0}^{N-1} x(iT_s) \exp(-2j\pi im/N) \right| \right]^2, \tag{32}$$

where T_s is the sampling period, N is the number of signal samples and $m\nu_0$ is the frequency, which is a multiple of a basis frequency ν_0. In Fig. 19 are presented the graphical representations of the noise and useful signal PSD (power of 30 dB m). The PSD is com-

S1051-2004(05)00090-4/FLA AID:588 Vol.●●●(●●●) ydspr588 [DTD5] P.16 (1-20)
YDSPR:m1a v 1.42 Prn:3/08/2005; 10:48 by:Vita p. 16

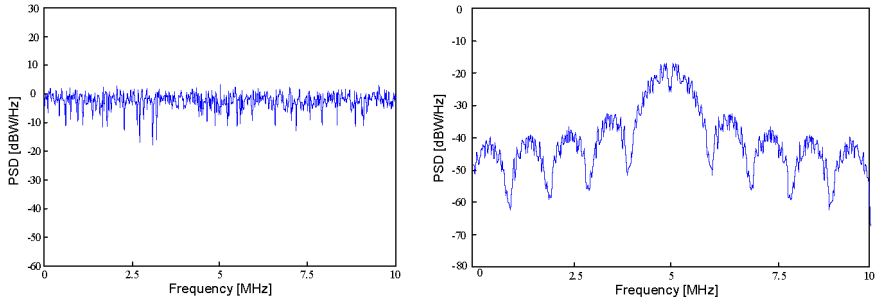

Fig. 19. PSD of (a) 0 dB W Gaussian noise and (b) useful data (SNR $= -10$ dB).

puted using a 20 MHz sampling frequency, and useful data are modulated around the intermediate frequency of 5 MHz.

5. Performances and analysis obtained with the Simulink simulator

Complete results about the ADP are presented in [10,11]. In all the simulations, the input SNR minimal value is set to -23 dB or below. The jammers are located in the spectral range of the useful data [1–10 MHz] with a JNR between 10 and 30 dB.

Measurements are made upon different scenarios to prove the ability of the FADP filter to respond properly in any case. Figures 20–22 show graphically the PSD (32) at the input and output of the FADP filter for one jammer (the CWI, PWI, and chirp, respectively). The following parameters have been considered: sampling frequency of 20 MHz, IF of 5 MHz, noise at 30 dB m, SNR of -10 dB. Figure 23 shows the same results with 15 jammers (the same parameters have been considered as in the previous case). These results prove that FADP efficiency remains the same whatever the number of jamming signals present in the spectrum is. In all the cases, the jammers are completely removed. The output noise power is not exactly the same as the input one because the signal passes through several AGC blocks, which can add a gain to the global signal. The main advantage of the FADP filter is to behave identically with one or many of them.

Table 1 is a numerical and complete summary of what could be observed in the figures above. Ten scenarios with 1 up to 15 jammers are presented. The FADP results are compared with the best ADP results obtained in Simulink in the same conditions. Measurements of SNR and JNR are made at the input and output of the FADP filter (26). The processing gain (30) and the SNR loss (31) are specified in each situation.

Before analyzing the results, it is important to precise that power measurement in a complex signal is hard to realize precisely. Then, every SNR or JNR measurement is given with a ± 1 dB range of uncertainty, particularly when JNR is close to 0. To make a comparison, ADP measurements are made in scenarios 1–6. For these tests, FADP performances are even better than ADP performances for CWI (tests 1 and 2) and slightly better for other jammers (tests 3–5). ADP performances decrease sensitively when 4 CWI are submitted at the input, whereas FADP behavior remains effective (test 6). SNR losses are a little bit

S1051-2004(05)00090-4/FLA AID:588 Vol.●●●(●●●) ydspr588 [DTD5] P.17 (1-20)
YDSPR:m1a v 1.42 Prn:3/08/2005; 10:48 by:Vita p. 17

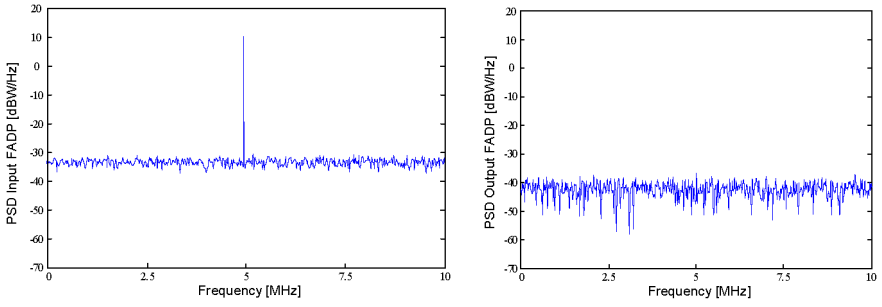

(a) (b)

Fig. 20. Input and output PSD with a CWI jammer (frequency of the jammer $f_j = 5$ MHz, with JNR = 20 dB).

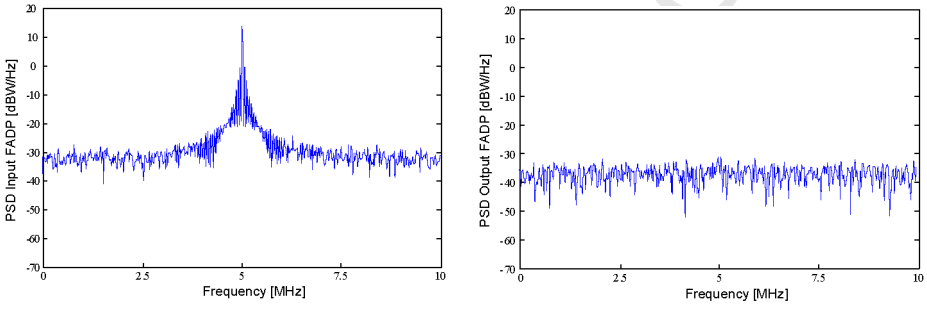

(a) (b)

Fig. 21. Input and output PSD with a PWI jammer (frequency of the jammer $f_j = 5$ MHz, with JNR = 20 dB).

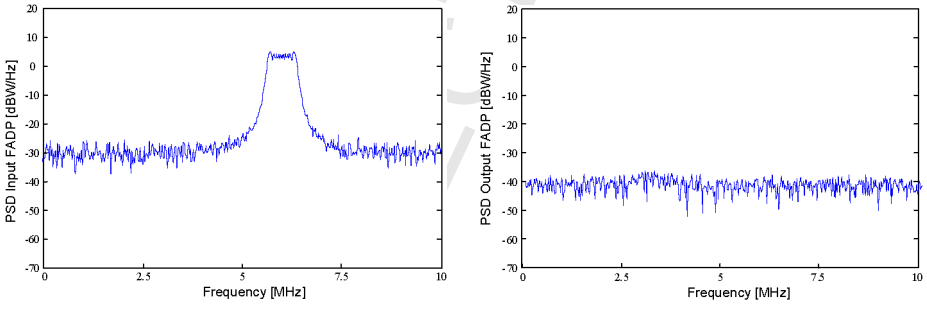

(a) (b)

Fig. 22. Input and output PSD with a chirp jamming signal (frequencies of the jammer $f_j = 5$–7.5 MHz, with JNR = 20 dB).

more important in the case of jammers centered in the main lobe (tests 1 and 3). But with any kind of jammers, the output JNR is small enough for tests 1–6.

Tests 7–10 were not effective with the ADP filter ("–" in the table means that the techniques used to measure ADP output SNR and JNR do not enable to obtain consistent

S1051-2004(05)00090-4/FLA AID:588 Vol.●●●(●●●) ydspr588 [DTD5] P.18 (1-20)
YDSPR:m1a v 1.42 Prn:3/08/2005; 10:48 by:Vita p. 18

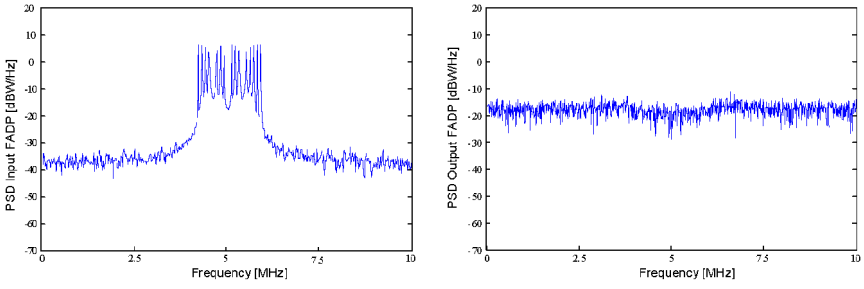

(a) (b)

Fig. 23. Input and output PSD with 15 CWI centered in the main lobe of GPS signal (4.3 MHz $\leqslant f_j \leqslant$ 5.7 MHz, with a global JNR = 27 dB).

Table 1
Comparative performances of ADP and FADP filter in several situations

Sort of interference	Inputs		ADP outputs		FADP outputs			
	SNR_{in} (dB)	JNR_{in} (dB)	SNR_{out} (dB)	JNR_{out} (dB)	SNR_{out} (dB)	JNR_{out} (dB)	Processing gain (dB)	SNR loss (dB)
1 CWI (4.7 MHz)	−23	20	−27.0	8.0	−24.8	0.7	19.4	−1.8
1 CWI (2.1 MHz)	−23	20	−23.4	8.0	−23.0	0.0	20.0	0.0
1 PWI (4.9 MHz)	−23	20	−23.8	5.5	−23.9	5.3	15.0	−1.5
1 PWI (2.1 MHz)	−23	20	−23.0	3.3	−23.0	3.5	16.5	0.0
1 chirp (5000 points 2–6 MHz)	−23	20	−23.6	2.3	−23.0	1.9	18.1	0.0
4 CWI	−23	20	−25.3	9.0	−25.8	1.0	19.0	−2.8
2 CWI, 1 chirp, and 1 PWI	−23	20	–	–	−27.5	5.8	14.1	−4.6
5 CWI and 5 PWI	−10	24	–	–	−17.5	11.5	12.5	−7.5
10 CWI	−10	25	–	–	−17.2	9.5	15.5	−7.2
15 CWI	−10	27	–	–	−19.4	9.0	17.0	−9.4

results) but FADP filter could still achieve good performances. The output JNR is more important but the input JNR increases too. An increase of SNR loss is due to the important number of jammers, as most of them are located in the main lobe of the useful data signal (between 4 and 6 MHz). This is the reason why the output useful data signal is affected. Some tests have been already realized with the FADP filter inserted in a global GPS receiver simulator. In the presence of the filter, the input JNR can be increased of 20 dB W. Other anti-jamming techniques of post-correlation, like spectral dispreading enable to manage a JNR of 10 dB at the output of the FADP filter.

Eventually, correlation loss has been measured in the absence of the jammer. A normalized input signal including a Gaussian noise (power of 30 dB m) and useful data drowned in the noise (SNR between −10 and −23 dB) is submitted at the input of the FADP filter. The FADP output is also normalized. Values of useful data and signal crosscorrelation peaks are measured before and after the filter. Correlation losses obtained are located between 0 and −0.4 dB, as a function of the input SNR. This proves that the FADP filter lets the useful data signal intact when it passes through the filter.

S1051-2004(05)00090-4/FLA AID:588 Vol.●●●(●●●) ydspr588 [DTD5] P.19 (1-20)
YDSPR:m1a v 1.42 Prn:3/08/2005; 10:48 by:Vita p. 19

6. Conclusions

One of the main concerns with the use of the GPS and other positioning systems is the ability to operate in all conditions and to maintain integrity in hostile environment. In this paper, we have shown that the FADP filtering could open new horizons in digital anti-jamming techniques. Digital processing in the FADP filter is pretty close to the ADP filter; no important changes being necessary except the addition of the FFT and IFFT blocksets. Then, measurement techniques have been the object of great thinking to be able to work as precise as possible in real conditions. In the presence of one or two jammers, the performances of the FADP filter are equivalent to those of the ADP filter. In the presence of more jammers, the FADP filter has shown to be more effective than the ADP one. Spectral processing enables to eradicate precisely all sorts of jammers, like PWI, CWI and chirp, whose frequencies are located in the main lobe of a GPS Gold sequence. JNR is reduced from at least 12 up to 20 dB when passing through the filter. Correlation loss, measured in absence of jammers, is under 0.5 dB in any case.

Further investigations will be done with the FADP filter inserted in an entire GPS/GALILEO receiver Simulink model, in order to study its impact on the performances of the receiver. The simulation that we have evocated here with Simulink has been developed in order to be easily translated and implemented in a FPGA component. Real-time proof of concept demonstrator has been designed to be inserted in real GPS receiver in order to measure real performance of such a filter. Moreover, the great advantage of the FADP filter is its easy "plug-in" ability, enabling to insert it in any kind of CDMA receivers.

References

[1] A. Ndili, D.P. Enge, GPS receiver autonomous interference detection, in: IEEE Position, Location and Navigation Symposium—PLANS 98, Palm Spring, CA, 1998.
[2] R.J. Landry, Techniques de Robustesse aux Brouilleurs pour les Récepteurs GPS, in: Département d'Etudes et de Recherches en Automatique DERA/CERT et du Laboratoire Electronique et Physique, Toulouse, France, 1997, pp. 58–115.
[3] R.J. Landry, A. Renard, Analysis of potential interference sources and assessment of present solutions for GPS/GNSS receivers, in: Fourth St. Petersburg International Conference on Integrated Navigation Systems, St. Petersburg, 1997.
[4] F. Amoroso, Adaptive A/D converter to suppress CW interference in DSPN spread-spectrum communications, IEEE Trans. Commun. COM-31 (10) (1983) 1117–1123.
[5] R.J. Landry, V. Calmetes, M. Bousquet, Impact of interference on a generic GPS receiver and assessment of mitigation techniques, in: IEEE 5th International Symposium on Spread Spectrum Techniques and Applications Proceedings, vol. 1, 1998, pp. 87–91.
[6] E. Balboni, J. Dowdle, J. Przyjemski, Advanced ECCM techniques for GPS processing, AGARD 488 (1988) 3–12.
[7] J. Przyjemski, E. Balboni, J. Dowdle, B. Holsapple, GPS anti-jam enhancement techniques, in: Proceedings of 49th Annual Meeting on Future Global Navigation and Guidance, Cambridge, MA, 1993.
[8] J. Capon, Optimum coincident procedures for detecting weak signals in noise, IEEE Trans. Inform. Theory (1960).
[9] V.R. Algazi, R.M. Lerner, Binary detection in white non-Gaussian boise, in: MIT Lincoln Laboratory Report, vol. DS-2138, 1964.
[10] R. AbiMoussa, R.J. Landry, Anti-jamming solution to narrowband CDMA interference problem, in: Canadian Conference on Electrical and Computer Engineering, vol. 2, 2000, pp. 1057–1062.

S1051-2004(05)00090-4/FLA AID:588 Vol.●●●(●●●) ydspr588 [DTD5] P.20 (1-20)
YDSPR:m1a v 1.42 Prn:3/08/2005; 10:48 by:Vita p. 20

[11] R. AbiMoussa, Techniques de Robustesse aux Brouilleurs pour les Récepteurs GPS par un Traitement ADP, Ecole de Technologie Supérieure, Montreal, Master Memorandum, January 2001.
[12] P.Y. Arquès, Détection Avec Hypothèses Non Aléatoires, Décision en Traitement du Signal, Masson, 1982, pp. 154–160.
[13] D. Allinger, D. Fitzmartin, P. Konop, A. Tetewsky, P.V. Broekhoven, J. Veale, Theory of an adaptive non-linear spread-spectrum receiver for Gaussian or non-Gaussian interference, in: 12th Asilomar Conference on Signals, Systems and Computers, 1987.
[14] J.M. Malicorne, Approfondissement de la Technique ADP, ENSAE, Toulouse, France, September 1998.

René Landry Jr. was born in Montreal in 1968. He received a Bachelor Engineering degree at the Ecole Polytechnique of Montreal, Canada, in 1992, a Master of Science in satellite communication engineering at the University of Surrey, Guildford, England, in 1993, a Master in space electronics and a DEA in microwaves at the ENSAE/SupAero, Toulouse, France, in 1994. Professor Landry obtained his PhD degree at Université Paul-Sabatier, Toulouse, France, in 1997. He also has a Post Doc in Space Science at the National French Space Industry (CNES), Toulouse, France, in 1998. Since 1999, Professor Landry is involved in the problem of GPS/Galileo/Bluetooth Interferences for the Canadian Navigation and Communication Industries. His major interest concerns the development of new innovative mitigation techniques for GPS receiver robustness design including those of electronic inertial navigation system based on low cost MEMs. He is actually working on several digital signal processing applications in anti-jamming and inertial navigation systems.

Pierre Boutin was born in France in 1978. He received a diploma of Information Technology Engineer at the Ecole Polytechnique of Paris, France, in 2000, and a diploma of Computer Science Engineer at the Ecole Nationale Supérieure des Techniques Avancées of Paris, France, in 2002. In 2000, he was with Alcatel Optronics, Nozay, France. During 2000–2001, he was with France Telecom, Issy les Moulineaux, Paris. He has incorporated the Ecole de Technologie Supérieure of Montreal since 2002. His major interests include communication and digital signal processing.

Aurelian Constantinescu received an Aerospace Engineering degree from the Polytechnic University of Bucharest (Romania) in 1992. He has received also a Master degree in 1993 and a PhD degree in 2001 in control from the Polytechnic National Institute of Grenoble, France. He worked as a post-doctoral researcher at the Launch Division of the French Space Agency (CNES) in Evry, France, on the control of conventional launchers and, in particular on the Ariane 5 launcher. Since 2002 he is a post-doctoral researcher in the Electrical Engineering Department of Ecole de Technologie Superieure (ETS), Montreal, Canada. His research interests in the last 2 years include global navigation satellite systems (GPS and Galileo) and indoor positioning systems.